

# A Study on Energy Harvesting Through the Use of Electromagnetic Dampers in Motion Control Schemes

By

Geoffrey Bomarito

Bachelor of Science in Civil and Environmental Engineering

Cornell University, 2009

SUBMITTED TO THE DEPARTMENT OF CIVIL AND ENVIRONMENTAL ENGINEERING IN PARTIAL FULFILLMENT OF THE REQUIREMENTS FOR THE DEGREE OF

MASTER OF ENGINEERING IN CIVIL AND ENVIRONMENTAL ENGINEERING

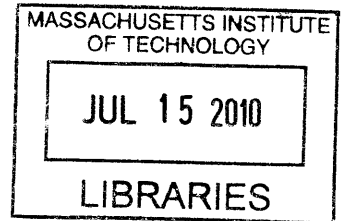
**ARCHIVES**

AT THE

MASSACHUSETTS INSTITUTE OF TECHNOLOGY

June 2010

© 2010 Geoffrey Bomarito. All rights reserved.



The author hereby grants to MIT permission to reproduce and to distribute publicly paper and electronic copies of this thesis document in whole or in part in any medium now known or hereafter created.

Signature of Author: \_\_\_\_\_

Handwritten signature of Geoffrey Bomarito in black ink.

Department of Civil and Environmental Engineering

May 7, 2010

Certified by: \_\_\_\_\_

Handwritten signature of Jerome J. Connor in black ink.

Jerome J. Connor

Professor of Civil and Environmental Engineering

Thesis Supervisor

Accepted by: \_\_\_\_\_

Handwritten signature of Daniele Veneziano in black ink.

Daniele Veneziano

Chairman, Departmental Committee for Graduate Students

# **A Study on Energy Harvesting Through the Use of Electromagnetic Dampers in Motion Control Schemes**

By

Geoffrey Bomarito

Submitted to the Department of Civil and Environmental Engineering on May 7, 2010 in Partial Fulfillment of the Requirements for the Degree of Master of Engineering in Civil and Environmental Engineering at the Massachusetts Institute of Technology.

## **Abstract**

In recent years, there is a trend in most fields toward more environmentally friendly products and processes. This trend toward sustainable living is often dubbed the “Green Revolution”. Because the Green Revolution is concerned with environmentally friendly ways of energy production, and structural engineering often has the task of controlling and dissipating energy, the logical step would be to unite the two concepts. This study investigates the use of the electromagnetic damper as an energy harvesting device in multiple damping schemes. It is shown that the use of the electromagnetic damper in a tuned mass damper scheme produces the most available energy to be harvested.

Thesis Supervisor: Jerome J. Connor

Title: Professor of Civil and Environmental Engineering

## **Acknowledgements**

I would like to thank my advisor Jerome Connor for his guidance and support. His willingness to provide assistance and enthusiasm for the subject have been inspirational.

I would like to thank Simon Laflamme for his support and assistance in the modeling processes of this study. He has proved to be an invaluable source of knowledge.

I would also like to thank Rogelio Palomera-Arias because his work on electromagnetic dampers was part of the inspiration behind this study.

I would like to thank my family and friends for their years of love and support, without which I would not be who or where I am today.

Thank you to Momo, K-Wob, MD, R Siebs, R-bex, J Hsiaw, Stievie M, J 'Toad' Mills, P-Town, Big C, and all the other MEng 2010 students for your help and for a great year.

# Contents

|       |   |    |
|-------|---|----|
| 1     | Introduction.....   | 6  |
| 1.1   | Motivation.....   | 6  |
| 1.2   | Framework and Scope.....                                    | 6  |
| 2     | Energy Harvesting Damping Devices.....                      | 8  |
| 2.1   | Introduction.....   | 8  |
| 2.2   | Piezoelectric Devices.....                                  | 8  |
| 2.3   | Electromagnetic Devices.....                                | 9  |
| 2.4   | Discussion and Selection.....                               | 11 |
| 3     | Motion Control of Structures.....                           | 12 |
| 3.1   | Introduction.....   | 12 |
| 3.2   | Traditional Inter-Story Damping.....                        | 12 |
| 3.3   | The Tuned Mass Damper.....                                  | 13 |
| 4     | Model.....  | 15 |
| 4.1   | The Electromagnetic Damper.....                             | 15 |
| 4.1.1 | Equivalent Damping and Pseudo Stiffness.....                | 16 |
| 4.1.2 | Available Energy.....                                       | 17 |
| 4.2   | Toy Structure.....  | 19 |
| 5     | Results.....  | 21 |
| 5.1   | Validation of Model.....                                    | 21 |
| 5.2   | Available Power Comparisons.....                            | 22 |
| 5.3   | Further Exploration.....                                    | 25 |
| 6     | Discussion.....   | 28 |
| 7     | Bibliography.....   | 29 |
| 8     | Appendix A: Other Assumptions Made in the MATLAB Model..... | 30 |

## List of Figures

|   |    |
|---|----|
| Figure 1: Geometry of a typical piezoelectric material with the top and bottom surfaces electroded and $x_3$ aligned with poling direction..... | 8  |
| Figure 2: Simplified Linear Electromagnetic Damper .....  | 10 |
| Figure 3: Transfer Function for Wind Excitation.....  | 13 |
| Figure 4: Effect of Tuned Mass Damper on Single Degree of Freedom System.....   | 14 |
| Figure 5: Prototype Magnetic Damper .....   | 15 |
| Figure 6: Dimensional Parameters of Electromagnetic Damper .....  | 15 |
| Figure 7: Dimensional and Magnetic Parameters of Electromagnetic Damper .....   | 16 |
| Figure 8: Damper Power Dissipation as a Function of Load Resistance.....  | 18 |
| Figure 9: Idealization of Traditional Inter-Story Damping .....   | 19 |
| Figure 10: Idealization of Tuned Mass Damper .....  | 19 |
| Figure 11: Validation of Response of EM Damper.....   | 21 |
| Figure 12: Validation of Power Dissipation Equations.....   | 22 |
| Figure 13: Relative Response of Inter-Story damping and TMD Schemes .....   | 23 |
| Figure 14: Available Power for the Inter-Story and Tuned Mass Damping Schemes.....  | 24 |
| Figure 15: Available Power for the Inter-Story and Tuned Mass Damping Schemes Normalized by Scale of Damping.....                               | 24 |
| Figure 16: Response of Tuned Mass Damper with Varying $\alpha$ .....  | 25 |
| Figure 17: Power Dissipation vs. $\alpha$ at $\Omega/\omega = 1.2$ .....  | 26 |
| Figure 18: Power Dissipation vs. $\alpha$ at $\Omega/\omega = 1.1$ .....  | 26 |
| Figure 19: Power Dissipation vs. $\alpha$ at $\Omega/\omega = 1.0$ .....  | 26 |
| Figure 20: Power Dissipation vs. $\alpha$ at $\Omega/\omega = 0.9$ .....  | 26 |
| Figure 21: Optimum $\alpha$ as a Function of Forcing Frequency Ratio .....  | 27 |

# **1 Introduction**

## **1.1 Motivation**

A major part of the field of structural engineering is motion control; buildings, bridges, and nearly every other structure must be designed to certain deflection limits under normal and extraordinary loadings. Some of these loadings are dynamic forces such as wind loads, and earthquake loads. These loads impart energy to the structure, which is stored as strain energy, potential energy, and kinetic energy. Unless this energy is dissipated somehow, the structure will continue to gain more energy and would eventually exceed its deflection limits. A well known example of this is the original Tacoma Narrows Bridge which collapsed in 1940 due to dynamic response caused by wind. It then becomes a structural engineering problem to understand the dynamics of these systems, and to control the structure's response. A common way of achieving this is to use devices called dampers; these devices dissipate energy to their surroundings.

In recent years, there is a trend in most fields toward more environmentally friendly products and processes. This trend toward sustainable living is often dubbed the "Green Revolution". The field of structural engineering has been greatly affected by this revolution; with the major areas of innovation in material use and construction processes. There is, however, one more area that is less developed: energy recapture.

Because the green revolution is concerned with environmentally friendly ways of energy production, and structural engineering often has the problem of having too much energy, the logical step would be to unite the two concepts. Ideally there would be some kind of system that could capture the energy of a structure and convert it into useable energy in the form of electricity.

## **1.2 Framework and Scope**

The basic approach to this research is twofold. Firstly, types of energy harvesting devices will be examined, namely piezoelectric devices and electromagnetic devices. These will

be discussed, and one will be taken for further examination. Secondly, schemes for installing these devices will be investigated. Based on the properties of the chosen damper a scheme will be decided as the more optimal way for capturing energy. Some further exploration will be done on this scheme.

The technology employed in these energy harvesting schemes will be more expensive than traditional dampers, but the goal of this work is to show that these devices may be more feasible if properly installed in an energy harvesting scheme. The energy will provide a payback on a higher initial investment. The immediate goal of this work is to provide a stepping stone for more research; research that will show the optimal use of these devices in energy harvesting schemes. This may, ultimately, prove the financial feasibility of these devices.

## 2 Energy Harvesting Damping Devices

### 2.1 Introduction

As previously stated, structures are imparted energy through external sources and must carry this energy. They do so by means of strain (deflection) energy, potential energy and kinetic (motion) energy. The goal of the preceding energy harvesting damping devices is to convert these energy types to something useable, such as electricity. The two devices discussed use different sources for the energy conversions. Piezoelectric devices are able to convert strain energy to electricity, and electromagnetic devices are able to convert kinetic energy to electricity. Each has its advantages and disadvantages.

### 2.2 Piezoelectric Devices

Piezoelectric materials are ones that efficiently convert strain energy into electricity. These special materials create a voltage under an applied strain; they also strain under an applied voltage. A general schematic of this type of material is shown in Figure 1. In this figure a current is applied to both top and bottom surfaces and as a result the material shrinks (in the  $x_2$  and  $x_3$  directions).

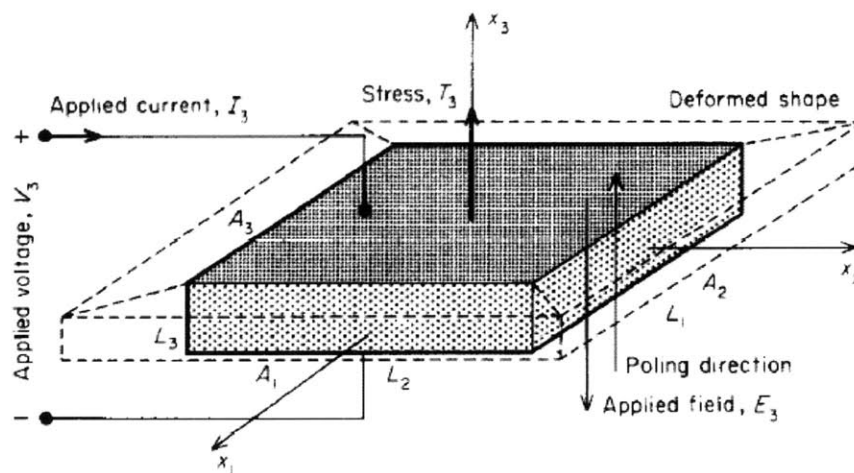


Figure 1: Geometry of a typical piezoelectric material with the top and bottom surfaces electroded and  $x_3$  aligned with poling direction (1)



Piezoelectric materials have been used in a wide range of applications from sensors and actuators in smart structures to active vibration suppression systems and even as structural damping devices (1). However, the work done on piezoelectric damping has come mainly in the form of passive electrical damping through use of electrical circuits, such as the work of Hagood and Flotow (1).

These devices, such as the ones explored in the work of Czarnecki (2), are made up of a few piezoelectric tiles mounted onto a member that will act in bending. This bending causes strain in the piezoelectric tiles which are in turn connected to an electrical circuit. In most cases this circuit consists of simply resistors that dissipate the electricity as heat. Theoretically this electricity could be captured and saved. The overall effect of the piezoelectric device on the bending member is one of passive damping.

Use of such piezoelectric schemes has many benefits. The piezoelectric devices could theoretically be placed anywhere on a structure, as long as that member will be strained. Because of this, these devices are very easy to put into existing structures. The devices are also easily attached to electric circuits, and offer very efficient conversion of energy.

Unfortunately there are also many drawbacks to this technology. In order to make the most of piezoelectrics they must be placed in places of higher strain, but in normal structures strains are very small. This limits the amount of energy that can be taken per each device. Also, the voltage produced by piezoelectric materials has a decay time, which makes the devices dependant on the rate of strain as well as the strain itself. As a result slow vibrations will provide little to no current in the circuit.

### **2.3 Electromagnetic Devices**

Electromagnetic devices involve the conversion of kinetic energy into electrical energy. A voltage is produced between two ends by the movement of a magnetic field. Figure 2 shows the simplified scheme of an electromagnetic damper.  $B$  is the magnetic field.  $I$  and  $R$  are the circuit current and resistance, respectively.

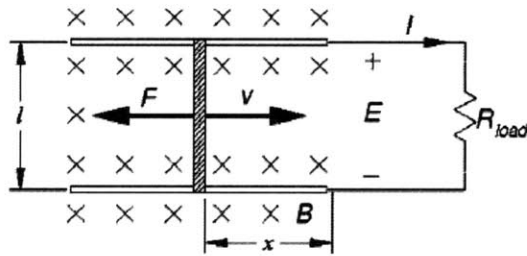


**Figure 2: Simplified Linear Electromagnetic Damper (3)**

The important things to note in this figure are that the force applied to the mover (with velocity  $v$ ) is in the opposite direction of its velocity. This movement also creates a current  $I$  in the circuit. The underlying physics behind this type of device is outlined below.

Using Faraday's law of induction, the induced electromotive force (voltage  $E$ ) is proportional to the derivative of the magnetic flux ( $\Phi_m$ ) through the circuit with respect to time.

$$E = -\frac{d\Phi_m}{dt}$$

where

$$\Phi_m = \int \vec{B} \cdot d\vec{A}$$

And where  $\vec{B}$ =magnetic field through the surface; and  $d\vec{A}$ =vector perpendicular to the surface whose magnitude=area element  $dA$ .

The force  $\vec{F}$  generated on a conductor segment of length  $d\vec{l}$  in the presence of a magnetic field  $\vec{B}$  is quantified by Lorentz law:

$$d\vec{F} = Id\vec{l} \times \vec{B} \quad (4)$$

If a constant velocity is taken, the resulting current ( $I$ ) and force ( $F$ ) are both linear scalings of that velocity. The magnitudes of these scaling factors are dependent on the geometry and materials of the machine.

The physics and construction of these electromagnetic devices is well developed, and has been a developing area of research. Most often they are used as actuation or as regenerative devices. The regenerative devices are most often found in automotive applications such as the regenerative braking systems in new hybrid vehicles (5), but they can also be found in applications such as powering offshore weather buoys (6). Application of structural regenerative dampers is, however, currently limited to theoretical studies, numerical simulations, and small scale tests (3).

The most critical advantage to this kind of damper is that so much has been done with it already. The idea has been substantially more refined than that of the piezoelectric scheme. Conversely, the size of the electromagnetic devices are much larger than that of the piezoelectric devices, this may in turn be a limiting factor of the design of large scale electromagnetic dampers.

## **2.4 Discussion and Selection**

Both of these technologies will be more expensive than the standard viscous dampers (the industry standard), but further advances and development may change that fact. The electromagnetic damper is pursued further in this study because it is definitely more feasible in this application. Though the piezoelectric devices are convenient in installation, they lack the scale needed in large structures. Electromagnetic dampers are much more feasible on large scale apparatus; they have already been put into automotive scale, while the piezoelectrics lack any large scale developments. Based on these reasons electromagnetic dampers will be focused on for the remainder of this report.

## 3 Motion Control of Structures

### 3.1 Introduction

In recent years design of structures based on motion, or deflections, has become more popular. In many cases structures are limited by these deflection limits rather than strength constraints. Countries such as Japan have been on the forefront of this motion based design, due mainly to high seismic activity.

High slenderness and sizeable loadings makes tall buildings some of the most concerned with this motion based design. Because of the height of these buildings and large windward areas, wind loading is usually the driving force in design of tall buildings. This study will focus primarily on tall buildings under wind loading. Furthermore, it will focus on two specific methods of motion control: traditional inter-story damping, and tuned mass dampers.

### 3.2 Traditional Inter-Story Damping

In Traditional inter-story damping, dampers are placed between each (or selected) floors of tall buildings. These dampers reduce the motion between the two floors in which they act; and jointly reduce the total deflection of the building. These dampers reduce total deflections by dissipating energy.

Often in structural dynamics, the effect of similar dampers on a system is shown through a transfer function, plotted against the excitation frequency. This transfer function is so named because it shows the relationship between the amount of force input into a system and the response of the system (i.e. how much of the force is transferred to motion). Figure 3 shows the relevant transfer function for excitation by wind which can be expressed as:

$H_1 = \frac{1}{\sqrt{(1-\rho^2)^2 + (2\xi\rho)^2}}$  where  $\rho$  is the ratio of forcing frequency ( $\Omega$ ) to the natural frequency of the structure ( $\omega$ ) and  $\xi$  is related to the amount of damping in the structure.

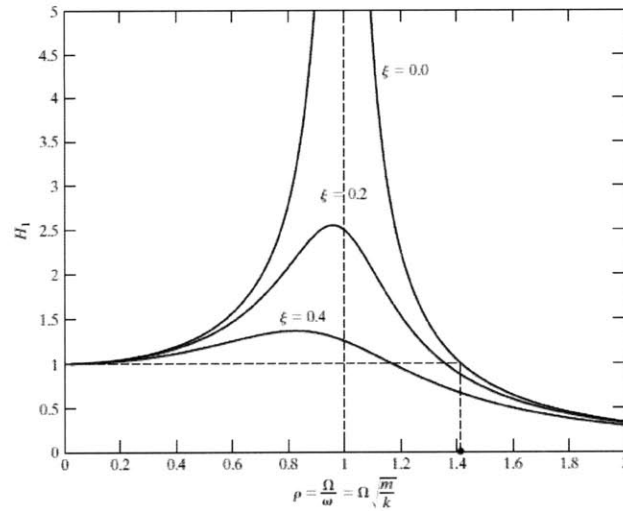


**Figure 3: Transfer Function for Wind Excitation (7)**

Things to note in this figure are the following:

- When damping (noted here as  $\xi$ ) is zero, the response is infinite under excitation at the structure's natural frequency ( $\Omega/\omega=1$ )
- When damping is added the response decreases everywhere
- The effect of damping is most notable at the natural frequency of the building

Transfer functions of this sort are useful in motion based design; they enable designers to adjust damping and other factors to produce a system that has a desired response.

### 3.3 The Tuned Mass Damper

More recently there has been other suggested ways of controlling motion; one of which is a tuned mass damper. A tuned mass damper (TMD) is a device made up of a mass, a spring, and a damper that is attached to a structure resulting in a reduced dynamic response of the structure. The TMD is tuned to a specific frequency so that when that frequency is excited, the damper will resonate out of phase with the structure's motion. (7) Implicit in this definition is the fact that this damper will only be effective for a certain frequency range; this is why the

damper must be tuned. Outside this range the response will be nearly unaffected. Figure 4 shows an example of the effect a tuned mass damper can have on a system.

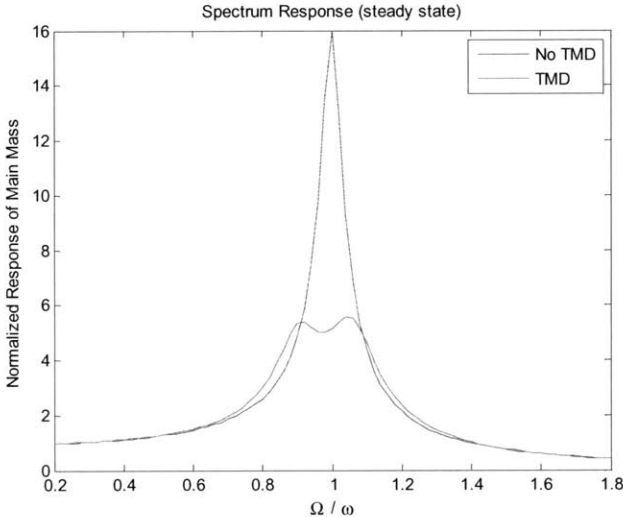


**Figure 4: Effect of Tuned Mass Damper on Single Degree of Freedom System**

The exact mechanics of the tuning process are beyond the scope of this paper, but in further modeling and analysis the tuned mass dampers are designed to the optimum specifications (given a certain mass ratio) as outlined in (7).

## 4 Model

### 4.1 The Electromagnetic Damper

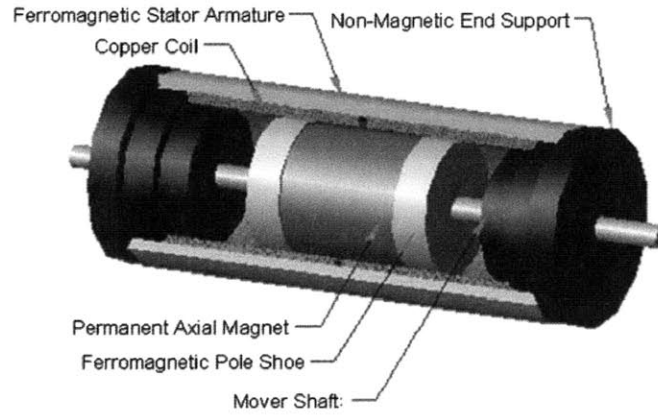


Figure 5: Prototype Magnetic Damper (4)

The electromagnetic damper used in this study is an extension of the prototype model posed by Palomera-Arias (3) which is shown here in Figure 5 through Figure 7. These figures illustrate the parameters necessary for the analysis of this prototype damper.

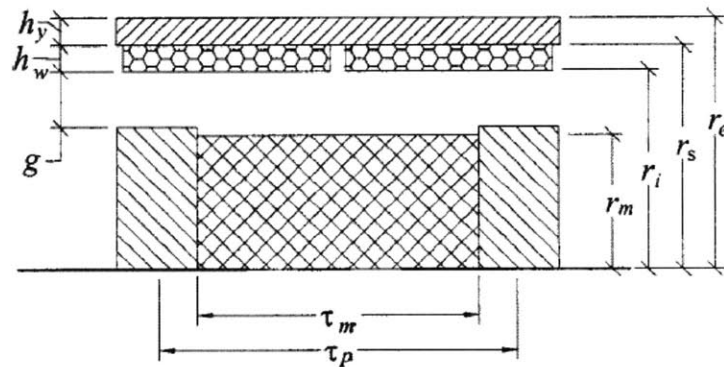


Figure 6: Dimensional Parameters of Electromagnetic Damper (4)

| Name                  | Symbol      | Description   |
|-----------------------|-------------|---|
| Pole pitch            | $\tau_p$    | The distance between adjacent pole shoes or radial magnets  |
| Magnet length         | $\tau_m$    | Actual length of the magnets                                |
| Pole shoe width       | $\tau_f$    | The width of the pole shoes: $\tau_f = \tau_p - \tau_m$     |
| Air gap thickness     | $g$         | The distance between the mover and the armature windings    |
| Number of poles       | $p$         | Even number of poles in the machine                         |
| Coil height           | $h_w$       | Height of the coils in the armature                         |
| Coil width            | $\tau_w$    | Width of each coil in the armature                          |
| Wire radius           | $r_w$       | Radius of the coil wire                                     |
| Coil turns            | $N_w$       | Number of turns on each coil                                |
| Active coil turns     | $N_a$       | Turns on each coil intercepted by the pole shoe flux        |
| Mover radius          | $r_m$       | Radius to the outside surface of the magnets or pole pieces |
| Armature radius       | $r_i$       | Radius to the inside surface of the armature                |
| Stator yoke radius    | $r_s$       | Radius to the inside surface of the stator yoke or shell    |
| Machine radius        | $r_e$       | Radius to the outer surface of the armature or stator yoke  |
| Yoke thickness        | $h_y$       | The thickness of the armature shell                         |
| Permeability          | $\mu_0$     | Permeability of free space, a constant                      |
| Relative permeability | $\mu_{Fe}$  | Relative permeability of iron used                          |
| Recoil permeability   | $\mu_{rec}$ | Magnet hysteresis loop slope approximation                  |
| Remanence             | $B_{rem}$   | Magnet residual flux density                                |

**Figure 7: Dimensional and Magnetic Parameters of Electromagnetic Damper (4)**

The paper also derives a few equations that are of particular interest to this study. Firstly, a variable known as the machine constant ( $K_t$ ) is defined.

$$F = K_t i_{circ}$$

where  $F$  is the force produced by the machine and  $i_{circ}$  is the current in the circuit of the machine.  $K_t$  is developed as:

$$K_t = \frac{\pi r_m^2 N_a B_{rem} \tau_m}{\tau_m \tau_f + r_m^2 \frac{\mu_{rec}}{\mu_0} \left( \ln \left( \frac{r_s}{r_m} \right) + \frac{1}{2\mu_{Fe}} + \frac{\tau_p \tau_f}{\mu_{Fe} h_y (r_s + r_e)} \right)}$$

and is a function of the geometric and magnetic parameters of the prototype machine.

#### 4.1.1 Equivalent Damping and Pseudo Stiffness

Secondly, Palomera-Arias develops further an equation for the force on the damper. If a harmonic velocity profile of  $v = \hat{v} \cos(\omega t)$  is assumed then

$$F = \beta K_t e^{-\left(\frac{R_{coil} + R_{load}}{L_{coil}}\right)t} + \frac{K_t^2}{\sqrt{(R_{coil} + R_{load})^2 + (\omega L_{coil})^2}} \hat{v} \cos(\omega t + \varphi)$$



where  $\beta$  depends on the initial conditions and  $\varphi = \tan^{-1}\left(-\frac{\omega L_{coil}}{R_{coil}+R_{load}}\right)$ .  $R_{coil}$  is the total resistance of the coil of the solenoid in the prototype (this value is fixed in a given machine).  $R_{load}$  is the external resistance that is added to the circuit, in this study this would be the energy capture apparatus.  $L_{coil}$  is the inductance of the coil.

The transient term will be neglected in further development of this equation.

The displacement profile is assumed:  $u = \frac{\hat{v}}{\omega} \sin(\omega t) = \hat{u} \sin(\omega t)$ . Now, if the cosine term is expanded and total circuit resistance ( $R_{circ}$ ) is taken as  $R_{load} + R_{coil}$  it follows that

$$F = \frac{K_t^2 \hat{v}}{(R_{circ})^2 + (\omega L_{coil})^2} [R_{circ} \cos(\omega t) + \omega L_{coil} \sin(\omega t)]$$

Next this equation is put into the familiar form  $F = c_{eq}v + k_{eq}u$ , which gives

$$c_{eq} = \frac{K_t^2 R_{circ}}{(R_{circ})^2 + (\omega L_{coil})^2}$$

and

$$k_{eq} = \frac{K_t^2 \omega^2 L_{coil}}{(R_{circ})^2 + (\omega L_{coil})^2}$$

where  $c_{eq}$  and  $k_{eq}$  are the equivalent damping and equivalent pseudo stiffness, respectively. This value of  $c_{eq}$  will be used as the damping values in the design of both the tuned mass damper and traditional schemes.

#### 4.1.2 Available Energy

The goal of this study is in determining which of two motion control schemes allows for the greater amount of energy to be harvested from the structure. For the purposes of this study it will be sufficient to look at the energy dissipated over  $R_{load}$ . This resistance would be the equivalent resistance of connecting the circuit to an energy storage medium; therefore, the energy across this resistance would be the upper bound of the energy that could be captured (henceforth referred to as available energy).

From Ohm's law it can be found that  $P_{load} = R_{load}i_{circ}^2$ . And Palomera-Arias (3) derives for an instantaneous velocity  $v$

$$i_{circ} = \frac{K_t v}{R_{circ}}$$

Which leads to

$$P_{load} = R_{load} \left( \frac{K_t v}{R_{circ}} \right)^2$$

The integral of this power over time is the available energy, but for the purposes of this study the available power will be a sufficient indicator of the amount of available energy.

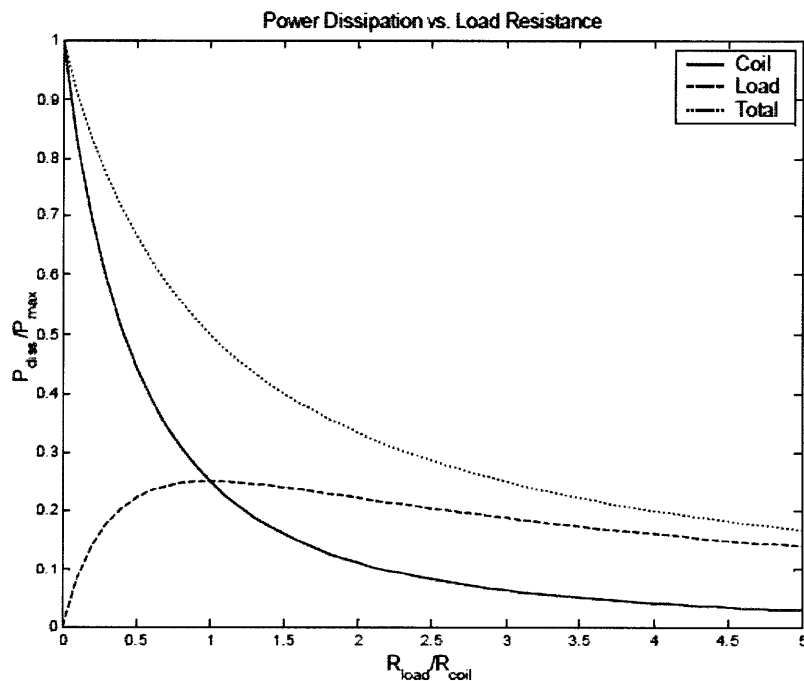


**Figure 8: Damper Power Dissipation as a Function of Load Resistance (3)**

Figure 8 shows the amount of power dissipated over the two resistances given a constant velocity and varying  $R_{load}$ . Henceforth the ratio of  $R_{load}/R_{coil}$  shall be referred to as  $\alpha$ . Because the focus of this study is on available power over  $R_{load}$ , an  $\alpha$  value of 1 is used in simulations to maximize  $P_{load}$ .

## 4.2 Toy Structure

To model the structure that these devices will work on, certain simplifications were made. Firstly, a single degree of freedom system was used, this is valid assuming that the response of the structure is mainly in the fundamental mode (i.e. higher modes are neglected in this study). Secondly, the structure is assumed to have no damping of its own, so all damping would come from the electromagnetic damper.

Figure 9 shows the idealization of the traditional inter-story damping scheme. This scheme also assumes proportional damping and so all damping can be idealized as a single damper.

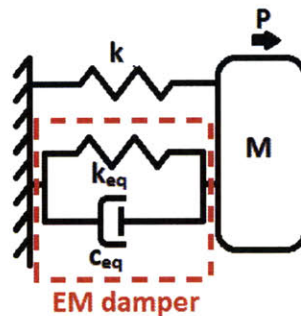


Figure 9: Idealization of Traditional Inter-Story Damping

Here  $M$  is the mass of the structure,  $k$  is the stiffness of the structure,  $p$  is the forcing function which will take the form of  $p = \hat{p} \cos(\Omega t)$ .

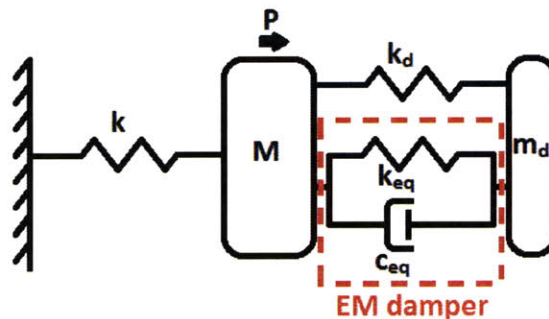


Figure 10: Idealization of Tuned Mass Damper

Figure 10 shows the idealized tuned mass damper scheme;  $m_d$  is the mass of the damping mass, and  $k_d$  is the stiffness of the tuned mass damper.

It should be noted that during analysis of these models the true physics of the electromagnetic damper is modeled (not simply as a spring and dashpot system). The  $k_{eq}$  and  $c_{eq}$  values are only used for the design of the dampers (in order to optimize the tuned mass damper and achieve a certain fraction of critical damping), but not in the dynamic simulation of the structure. Other assumptions made in the model are provided in Appendix A.

## 5 Results

### 5.1 Validation of Model

To show the validity of the model two tests were done. A model with the electromagnetic damper was compared to a model with a viscous damper. A viscous damper is used as a comparison because it is the industry standard and has been well studied. Figure 11 shows the comparison of a tuned mass damper scheme with the electromagnetic damper, and the same system with a viscous damper replacing it. The  $c$  value of the viscous damper is set equal to the  $c_{eq}$  of the electromagnetic damper. As expected, there little to no difference between the two plots; this validates the use of  $c_{eq}$  in design. Also note:  $\Omega$  is the forcing frequency and  $\omega$  is the natural frequency of the structure alone.

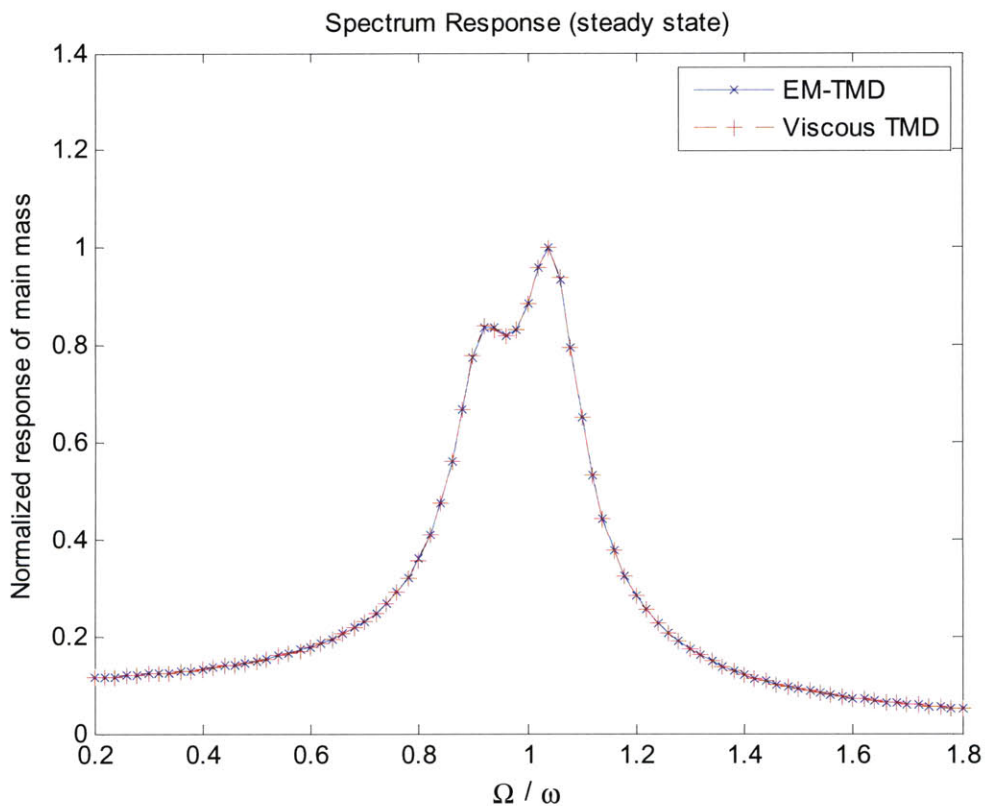


**Figure 11: Validation of Response of EM Damper**

The next validation test confirms the use of the power dissipation equation previously derived for the electromagnetic damper. This power dissipation is compared to the power

dissipated in a standard viscous damper which is known to be  $P = cv^2$ . Figure 12 illustrates these results, and once again the curves coincide.

Note: The total power dissipation is shown for the electromagnetic damper (i.e. the power dissipated over  $R_{coil}$  and  $R_{load}$ )

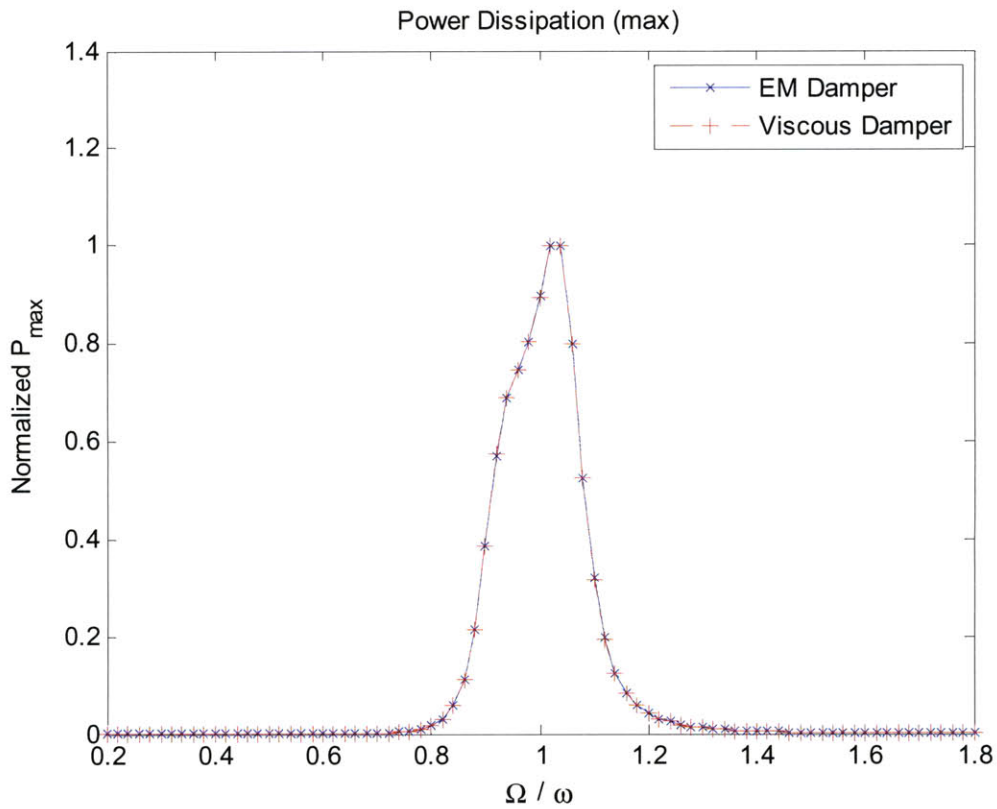
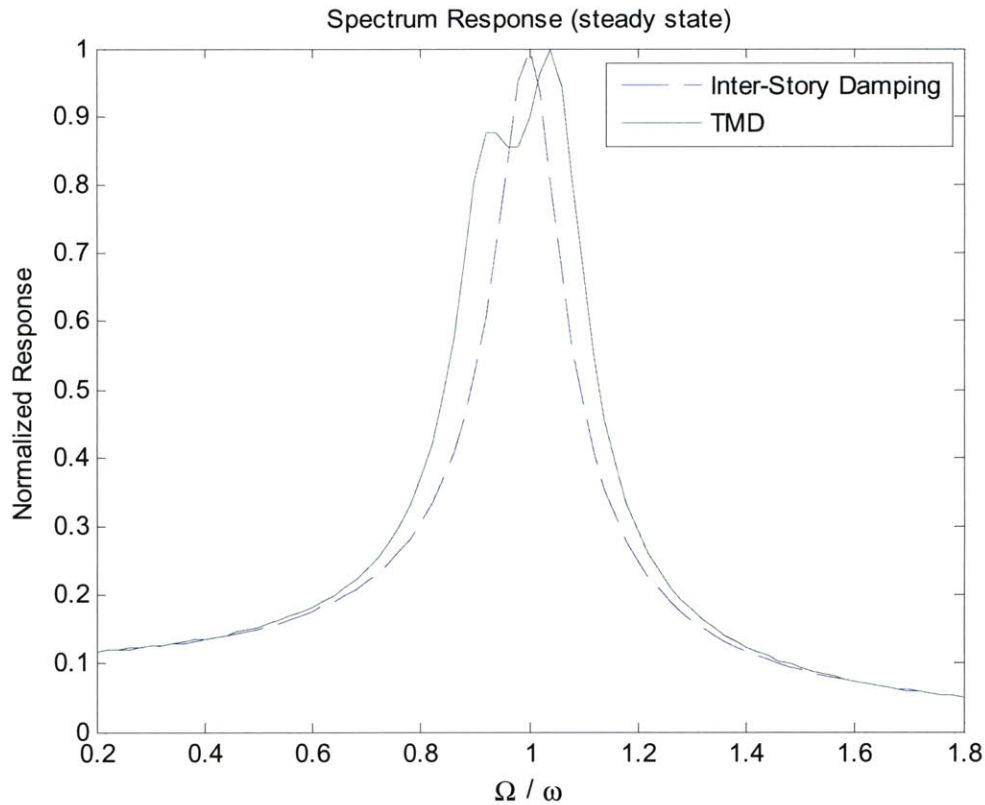


Figure 12: Validation of Power Dissipation Equations

## 5.2 Available Power Comparisons

In order to compare the two damping schemes (tuned mass damper and inter-story damping) it is first necessary to decide how they will be designed. In this study the two schemes were designed in order to have the same maximum response (i.e. they were designed using motion based design) and optimized from there. Figure 13 illustrates the response of the two schemes; note that the two schemes have the same maximum response.



**Figure 13: Relative Response of Inter-Story damping and TMD Schemes**

Based on these two schemes the maximum power of each scheme can be compared. The results of this are shown in Figure 14. The tuned mass damping scheme provides on the order of double the amount of power of the inter-story damping scheme. This difference in available power is further emphasized by the fact that more damping is required for the inter-story scheme. Figure 15 shows the same available power but normalized by the amount of damping; therefore, a relative 'damping per device is shown'. This shows that the available energy from the tuned mass damper scheme is more than an order of magnitude greater than that the other scheme. The tuned mass damper scheme is undoubtedly more efficient in energy harvesting using the electromagnetic damper than the traditional inter-story damping.

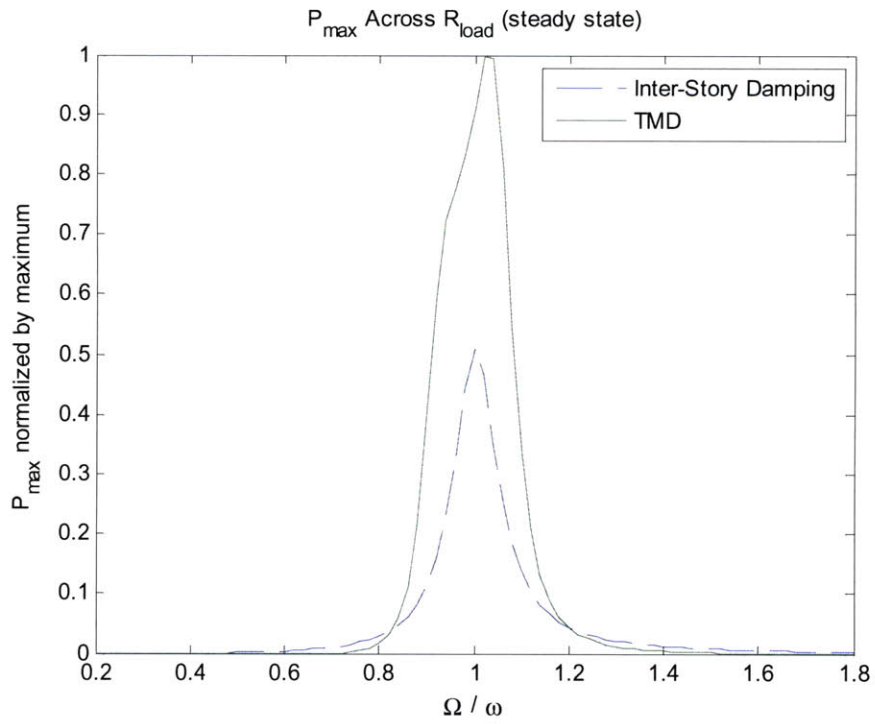


**Figure 14: Available Power for the Inter-Story and Tuned Mass Damping Schemes**

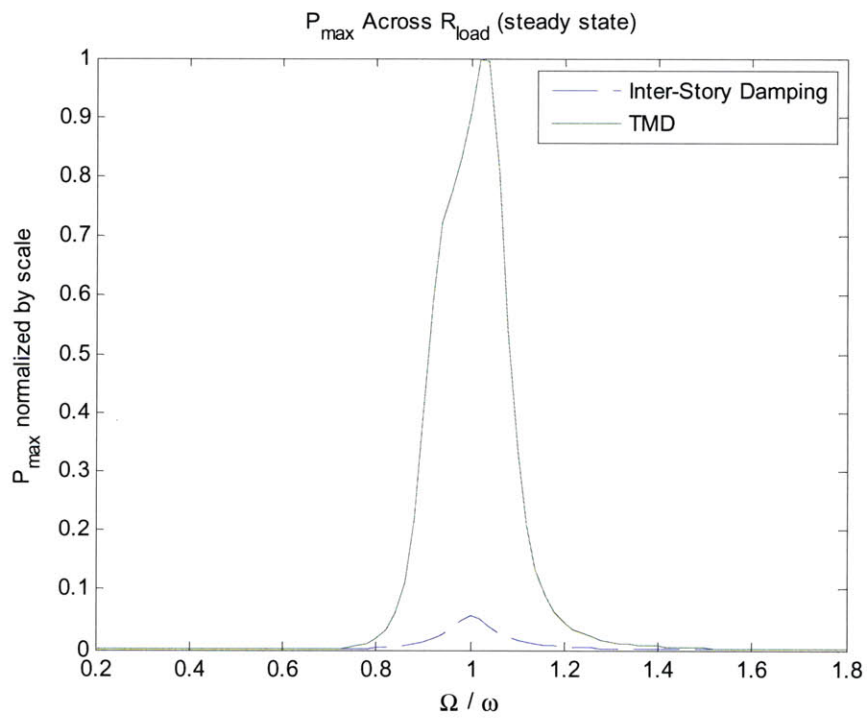


**Figure 15: Available Power for the Inter-Story and Tuned Mass Damping Schemes Normalized by Scale of Damping**



### 5.3 Further Exploration

Because the tuned mass damper was so much more efficient in energy harvesting, it was pursued further in order aid future research. Because the electromagnetic damper can be so easily manipulated with the addition of load resistance, this section is devoted to the exploration of the effects this has on both the response of the tuned mass damper and the available power.

As can be recalled from Figure 8, if a constant velocity is assumed the optimal  $\alpha$  value is 1, but as Figure 16 shows the response of the tuned mass damper is changed as  $\alpha$  varies. This has the implication of changing the velocity of the tuned mass damper which means the constant velocity previously assumed is no longer valid.

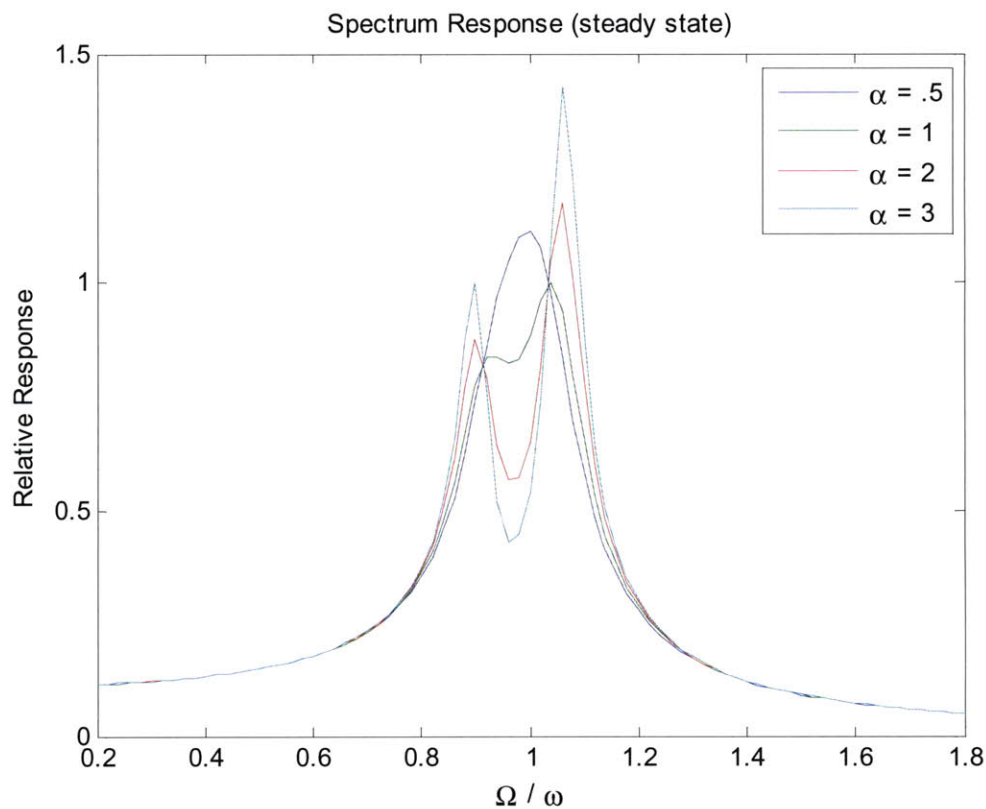


Figure 16: Response of Tuned Mass Damper with Varying  $\alpha$

Now if the experiment run in Figure 8 is repeated but with the variable velocity shown in Figure 16 new plots can be obtained. A few of these plots are shown in Figure 17 through Figure 19. These plots are the power dissipations as a function of  $\alpha$  at given frequency ratios ( $\Omega/\omega$ ).

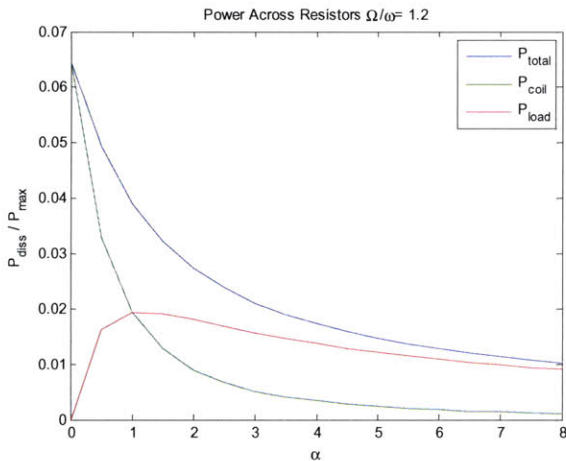


Figure 17: Power Dissipation vs.  $\alpha$  at  $\Omega/\omega = 1.2$

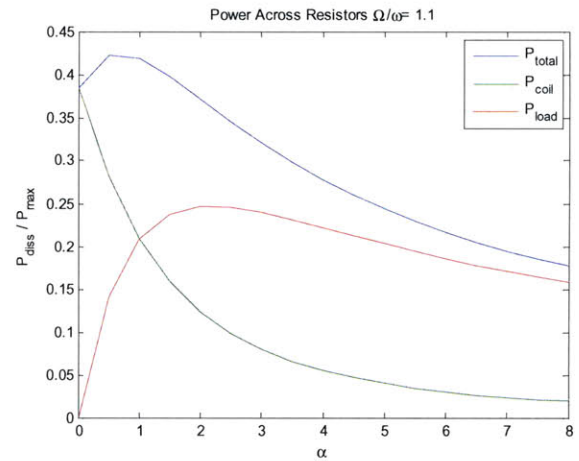


Figure 18: Power Dissipation vs.  $\alpha$  at  $\Omega/\omega = 1.1$

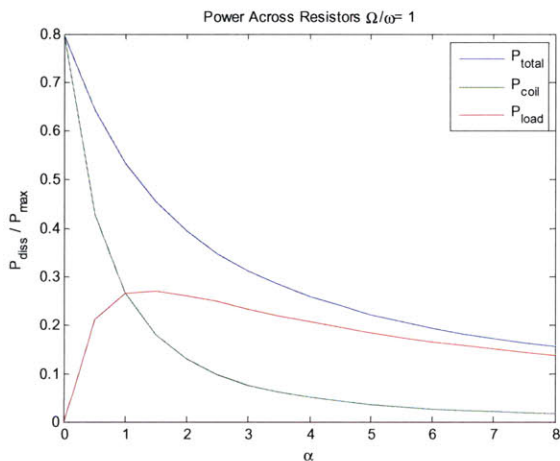


Figure 18: Power Dissipation vs.  $\alpha$  at  $\Omega/\omega = 1.0$

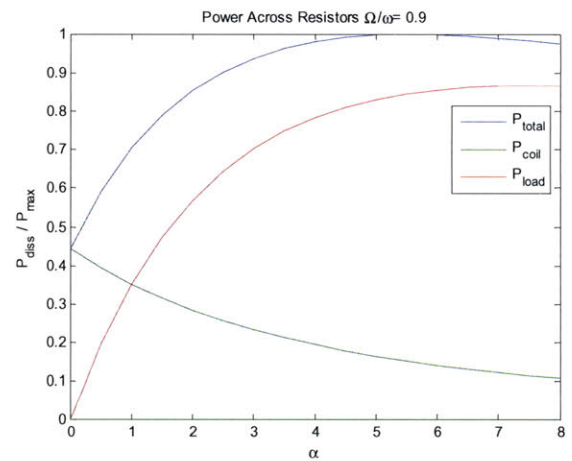
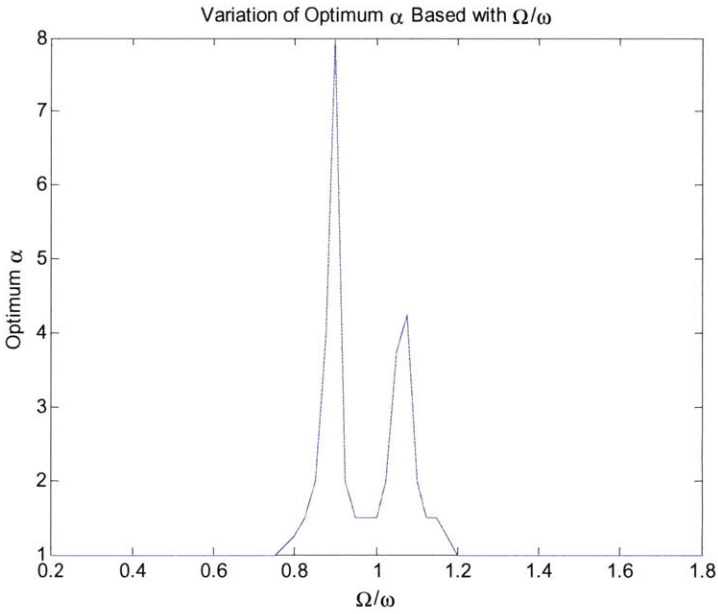


Figure 19: Power Dissipation vs.  $\alpha$  at  $\Omega/\omega = 0.9$

These figures show that there is indeed a difference between these variable velocity models and the constant velocity model used previously. The optimum  $\alpha$  for maximum available power (highest  $P_{load}$ ) varies depending on the frequency ratio of the excitation. Figure 20 shows the optimal  $\alpha$  as a function of frequency ratio. The optimum  $\alpha$  approaches 1 in

frequency ratios far from the resonant frequencies of the system; in these areas the variable velocity model approaches the constant velocity model. Near frequencies of resonance the optimum  $\alpha$  skyrockets, meaning that letting the damping mass move more will produce higher available power.



**Figure 20: Optimum  $\alpha$  as a Function of Forcing Frequency Ratio**

## 6 Discussion

As previously mentioned, the purpose of this study is to provide a stepping stone for future work. The ultimate goal would be to prove the feasibility of the electromagnetic damper as a way of harvesting energy from tall buildings. What can be taken from this study is that using an electromagnetic damper in conjunction with a tuned mass damper is an effective way of harvesting energy; however, this idea must be pursued further in order to show feasibility.

A study providing the quantification of this energy is the next logical step. As shown in Palomera-Arias's paper (4) the electromagnetic damper is substantially more expensive than the viscous dampers used today, but if this initial investment can be offset by an income from energy retrieval it may, indeed, prove to be a viable investment. As an extension of this energy capture scheme, a semi-active control scheme is also proposed. This scheme could maximize the amount of energy capture by adjusting the load resistance; this would also affect the response but this can be controlled as well. The semi-active scheme would increase the amount of energy harvesting with minimal investment and effort, further increasing the financial worth of the machines.

Finally, because the most expensive parts of these machines are the permanent magnets, a study is proposed that investigates the use of electromagnets instead of permanent magnets. The electromagnets would have to be powered by electricity, so a life cycle study must be done to quantify the energy needed and the financial benefit of using the cheaper electromagnets. These electromagnets may prove an even better investment if the energy harvesting scheme can provide a portion of the energy required to power the magnets.

As time passes and technology progresses, these electromagnetic dampers may eventually become financially competitive with other dampers; however, with motivation from the green revolution, coupled with the proposed energy harvesting schemes, the electromagnetic damper may rise in popularity at an even faster rate.

## 7 Bibliography

1. *Damping of Structural Vibrations with Piezoelectric Materials and Passive Electrical Networks.*

**Hagood, N.W. and Flotow, A. von.** 1991, Journal of Sound and Vibration, pp. 243-268.

2. **Czarnecki, Jerry J.** *A Structural Dynamics Design Methodology for the Optimization of Vibration to Electrical Energy Conversion in Piezoelectric Devices.* s.l. : Massachusetts Institute of Technology, 2010.

3. **Palomera-Arias, Rogelio.** *Passive Electromagnetic Damping Device for Motion Control of Building Structures.* Cambridge, MA : Massachusetts Institute of Technology, 2005.

4. *Feasibility Study of Passive Electromagnetic Damping Systems.* **Palomera-Arias, Connor, Jerome J. and Ochsendorf, John A.** 2008, Journal of Structural Engineering, Vol. 134, pp. 164-170.

5. *Analysis of a Regenerative Braking System for Hybrid Vehicles Using an Electro-Mechanical Brake.* **Ahn, J. K., et al.** 2009, International Journal of Automotive Technology, pp. 229-234.

6. **Cheung, Jeffrey T.** *Frictionless Linear Electric generator for Harvesting Motion Energy.* Thousand Oaks, CA : s.n., 2004.

7. **Connor, Jerome J.** *Introduction to Structural Motion Control.* s.l. : Pearson Education, Inc., 2003.

8. **Lindh, Cory W.** *Dynamic Range Implications for the Effectiveness of Semi-Active Tuned Mass Dampers.* Cambridge, MA : Massachusetts Institute of Technology, 2010.

## 8 Appendix A: Other Assumptions Made in the MATLAB Model

In order to accurately describe the values of  $L_{coil}$ ,  $K_t$ , and  $R_{coil}$  values used in the model a scaling of the prototype device created by Palomera-Arias was used. This is valid since the ratios of these values are of the most importance. The prototype is described in the figure below which is taken from (3).

| Group                       | Parameter (unit)                       | Value                 |          |
|-----------------------------|--|-----------------------|----------|
|                             |  | $k=0.5$               | $k=1$    |
| Overall Dimensions per Pole | Diameter (mm)                          | 131                   |          |
|                             | Length (mm)                            | 55.2                  |          |
|                             | Volume (m <sup>3</sup> )               | 7.43x10 <sup>-4</sup> |          |
| Air-Gap                     | Thickness (mm)                         | 1.0                   |          |
|                             | Layers                                 | 5                     |          |
| Coil Parameters             | Wire Diameter (AWG)                    | 15                    |          |
|                             | Turns                                  | 195                   |          |
|                             | Coil Height (mm)                       | 6.5                   |          |
| Magnet                      | Length (mm)                            | 25                    |          |
|                             | Radius (mm)                            | 51                    |          |
| Stator                      | Thickness (mm)                         | 7                     |          |
| Pole Shoes                  | Width (mm)                             | 15.1                  |          |
|                             | Circuit Resistance ( $\Omega$ )        | 0.422                 | 0.231    |
| Electrical                  | Inductance (mH)                        | 5.1                   |          |
|                             | Machine Constant (N/A)                 | 17.35                 |          |
| Damping per Pole            | (kN-s/m)                               | 0.652                 | 1.30     |
| Damping Density             | (kN-m <sup>-1</sup> s/m <sup>3</sup> ) | 871.5                 | 1743     |
|                             | Per Pole                               | \$103.66              |          |
| Cost                        | Damping                                | \$159.10              | \$79.55  |
|                             | Required Poles                         | 322                   | 161      |
|                             | Required Volume (m <sup>3</sup> )      | 0.24                  | 0.12     |
| Resulting Machine           | Effective Damping (kN-s/m)             | 0.242                 | 209.8    |
|                             | Machine Cost                           | \$33,382              | \$16,691 |